FIRST-PRINCIPLES AND CALPHAD-TYPE STUDY OF THE Ir-Mo AND Ir-W SYSTEMS

Y.-Y. Huang [a,b], B. Wu [a,*], F. Li [c,*], L.-L. Chen [b], Z.-X. Deng [b], K. Chang [b]

[a] Multiscale Computational Materials Facility, College of Materials Science and Engineering, Fuzhou University, Fuzhou, P. R. China
[b] Engineering Laboratory of Advanced Energy Materials, Ningbo Institute of Materials Technology and Engineering, Chinese Academy of Sciences, Ningbo, Zhejiang, P. R. China
[c] School of Materials Science and Engineering, Shanghai Jiao Tong University, Shanghai, P. R. China

Abstract

This study presents the thermodynamic modeling of the Ir-Mo and Ir-W systems by means of the CALPHAD (CALculation of PHAse Diagrams) approach supported with the first-principles calculations. A critical evaluation of the phase equilibria and the thermodynamic property data in literature was conducted for both systems. Due to the lack of experimental data, the first-principles calculations were applied to obtain the enthalpies of the solid and intermetallic phases. The thermodynamic parameters were assessed using the PARROT module of Thermo-Calc. A set of self-consistent parameters for the Ir-Mo and Ir-W systems was obtained after the optimization. Satisfactory agreement between the calculated results and the experimental data, including phase equilibria and thermodynamic properties was achieved.

Keywords: CALPHAD; Ir-Mo; Ir-W; Phase diagram; First-principles

1. Introduction

Iridium is widely used in the high-temperature applications [1-3] including crucibles and car engine spark plugs owing to its high strength and excellent corrosion resistance [4, 5]. However, the great brittleness [6, 7] of iridium metal restricts its application. Alloying of other elements (such as Mo, W and Th) can not only significantly improve its processability [8, 9] but also enhance its strength [10]. Moreover, the refractory metals (like Mo and W) with one of the most oxidation-resistant one (like Ir) would result in materials with particularly useful technological properties [11, 12]. Therefore, it is worthy to obtain a fundamental knowledge of the Ir-Mo and Ir-W systems, such as phase equilibria and thermodynamic data, for designing appropriate compositions of iridium-based alloys. Although limited experimental data on phase equilibria of the Ir-Mo and Ir-W systems have been reported [13-17], no thermodynamic information is available in literature. First-principles calculations have been widely accepted as a reliable method of predicting thermodynamic data for CALPHAD modeling when experimental data are lacking or have large uncertainties [18]; thus, we use it to obtain the enthalpies of the solid and intermetallic phases in both systems. In this paper the intention is to integrate the first-principles calculations and CALPHAD [19] modeling to assess the Ir-Mo and Ir-W systems.

2. Literature review
2.1 The Ir-Mo binary system

The Ir-Mo binary system consists of eight phases, including the Liquid, Fcc_A1, Bcc_A2 and five intermetallic compounds (IrMo$_3$, IrMo, Ir$_3$Mo, ε, σ). The structural information of the phases is listed in Table 1. In 1954, Raub [20] investigated the Ir-Mo alloys at temperatures ranging from 800 °C to 1600 °C using X-ray diffraction (XRD), and observed the IrMo$_3$ and ε phases. Later on, Knapton [21] applied the same method to study the Ir-Mo alloys covering 15 to 85 at.% Ir and discovered the σ phase. In 1963, Michalik and Brophy [15] constructed a phase diagram of the Ir-Mo system based on their experiments. Michalik and Brophy's samples were prepared with 99.9% Ir and 99.9% Mo powders and sintered in vacuum between 1200 °C and 1400 °C for an hour [15]. Only three intermetallic compounds (IrMo$_3$, ε and σ) were detected [15] with metallography, XRD, fluorescence, and electron microprobe analyses [15].

Five invariant reactions in this system were reported [15]: Liquid + Fcc_A1 ↔ ε at 2300 ℃, Bcc_A2 + Liquid ↔ IrMo₃ at 2110±10 ℃, Liquid + IrMo₃ ↔ σ at 2095±15 ℃, Liquid ↔ ε + σ at 2080±5 ℃ and ε ↔ σ + IrMo₃ at 1975±5 ℃. Furthermore, the solubility of Ir in Mo was determined as 16 at.% at 2110 ℃ and decreases to less than 5 at.% at 1500 ℃. The IrMo₃ phase transforms peritectically from Bcc_A2 and Liquid, at around 2110 ℃. The composition of this phase varies from 23 at.% Ir at 2110 ℃ to a range of 22-25 at.% Ir at 1900 ℃. The ℃ phase, is a stoichiometric compound, which transforms peritectically from the Liquid and IrMo₃ phases at about 2095 ℃. In the report of Michalik and Brophy [15], the ε phase can both appear in the eutectic and the eutectoid reactions, and it exists in a wide range from 37 at.% Ir at 2080 ℃ to 76 at.% Ir at 2300 ℃. The ε and Fcc_A1 two-phase region covers 76-78 at.% Ir at 2300 ℃. Besides, the lattice parameters of each phase were gained by their experiments [15], which are listed in Table 1. In 1965, Giessen [22] assessed the Ir-Mo binary system and proposed a new phase diagram. They added the IrMo and Ir₃Mo phases in the diagram based on literature data and their own experiments [22]. IrMo is a stoichiometric compound indicated as the low-temperature phase of ε. Furthermore, the Ir₃Mo phase was suggested to locate in the previous ε phase range [15]. Three more invariant reactions were included in the assessed phase diagram: Liquid + Fcc_A1 ↔ Ir₃Mo, ε ↔ IrMo + Ir₃Mo and ε ↔ IrMo + IrMo₃. The peritectic reaction Liquid + Fcc_A1 ↔ ε at 2300 ℃ summarized by Michalik and Brophy [15] was thus revised as Liquid+Fcc_A1 ↔ Ir₃Mo due to the appearance of Ir₃Mo. The invariant reactions are summarized in Table 2. Moreover, they measured the lattice parameters [22] of these two new phases using arc-melting, heat-treatments, metallographic, and X-ray powder-diffraction technique, as listed in Table 1.

2.2 The Ir-W binary system

The Ir-W binary system consists of seven phases including the Liquid, Fcc_A1, Bcc_A2, and four intermetallic compounds (IrW, Ir₃W, ε, σ). The structural information of the phases is listed in Table 1. In 1951, Raub and Walter [13] firstly investigated the intermediate phases after the sample annealing at 1400-1800 ℃ and observed the ε phase. The solidus and liquidus were studied by two research groups [14, 16] using the incipient melting technique and the drop method, respectively. Rapperport and Smith [14] used 99.9% pure Ir and W while Tylkina et al. [16] used 99.8% pure Ir and "high purity W" (as written in literature) to prepare the samples by arc melting. In 1991, Nagender et al. [23] assessed this system and suggested the existence of the Ir₃W and IrW phases

above 1200 ℃ with hexagonal and orthorhombic crystal structures, respectively. Recently, Omori et al. [17] verified the existence of the Ir₃W and IrW using the diffusion couple method and equilibrated alloys. In the latest assessed phase diagram [17], six invariant reactions exist: Liquid = ε + Fcc_A1, Liquid = ε + σ, Bcc_A2 + Liquid = σ, σ = ε + Bcc_A2, Fcc_A1 + ε = Ir₃W and ε =IrW + Bcc_A2. The eutectic reaction, Liquid = ε + Fcc_A1, appears at 2305 ℃ of 21 at.% W. The Fcc_A1 and ε two-phase region exists in the range of about 19~22 at.% W. Another eutectic reaction is Liquid = ε + σ appearing at 2460 ℃ of 70 at.% W. The content of W in the ε phase at 2460 ℃ is about 66 at.% [23]. The peritectic reaction, Bcc_A2 + Liquid = σ appears at 2540 ℃ of 75 at.% W and the content of W in the Liquid phase of this reaction is about 74 at.%. At 1810 ℃, the σ phase transforms into the ε and Bcc_A2 phases. The contents of W in the ε and Bcc_A2 phases are 57 at.% and 96 at.% in this eutectoid reaction, respectively. The assessed maximum solubility of Ir in W is about 10 at.% [23]. All the invariant reactions are summarized in Table 2.

3. First-principles calculations

Formation enthalpies obtained by the first-principles calculations can be considered as "experimental data" [26-29] when such data are unavailable. In the present work, the first-principles calculations were conducted in the Vienna *ab initio* simulation package (VASP) [30] with generalized gradient approximation (GGA) [31] proposed by Perdew et al. [32] for the exchange and correlation contributions, and the valence electrons were treated by projector augmented plane-wave (PAW) potentials [33]. When the Hellman-Feynman forces were less than 10^{-2} eV/Å, the atoms were deemed to be relaxed towards equilibrium. A plane-wave cutoff energy of 400 eV and an energy convergence criterion of 10^{-5} eV for electronic structure self-consistency were adopted to make the total energy difference less than 0.1 kJ/mol-atoms. The method of performing Brillouin-zone integrations was Monkhorst-Pack k-point [34] generation mesh scheme. The unit cell size and the ionic coordinates were fully relaxed to find the stable state. After the final static calculation, the formation enthalpies of compounds and end-members at 0 K can be described as following:

$$\Delta H_f(Ir_m X_n) = \frac{E(Ir_m X_n) - mE(Ir) - nE(X)}{m+n} \qquad (1)$$

Here the total energy of a compound or end-member is $E(Ir_m X_n)$ (X = Ir, Mo, W). The total energies of reference states for pure elements are E(X). Lattice parameters and mixing enthalpies of Fcc_A1 and Bcc_A2 Ir-Mo and Ir-W solid solutions were investigated using first-principles calculations utilizing the special

Table 1. Crystal structure data of the phases in the Ir-Mo and Ir-W systems

Phase	Structure type	Pearson symbol	Lattice parameter(Å)			Reference
		Space group	a	b	c	
Ir-Mo binary system:						
IrMo$_3$	β-W	Pm $\bar{3}$ n	4.959	4.959	4.959	[15]
			4.972	4.972	4.972	This work (cal.)
ε	hexagonal	P6$_3$/mmc	2.77	2.77	4.424	[15]
			2.795	2.795	4.463	This work (cal.)
IrMo	B19-MgCd	Pmcm	2.752	4.804	4.429	[22]
			2.752	4.804	4.429	This work (cal.)
Ir$_3$Mo	DO19-MgCd3	P6$_3$/mmc	5.487	5.487	4.385	[22]
			5.487	5.487	4.385	This work (cal.)
σ	hexagonal	P4$_2$/mnm	9.631	9.631	4.957	[24]
			9.705	9.705	4.957	This work (cal.)
Mo	cubic	Im $\bar{3}$ m	3.147	3.147	3.147	[15]
			3.173	3.173	3.173	This work (cal.)
Ir	cubic	Fm $\bar{3}$ m	3.839	3.839	3.839	[15]
			3.885	3.885	3.885	This work (cal.)
Ir-W binary system:						
e	hexagonal	P6$_3$/mmc	2.736	2.736	4.383	[13]
			2.808	2.808	4.485	This work(cal.)
s	hexagonal	P4$_2$/mnm	9.672	9.672	5.01	[21]
			9.749	9.749	5.018	This work(cal.)
Ir$_3$W	DO19-MgCd3	P6$_3$/mmc	5.496	5.496	4.39	[22]
			5.551	5.551	4.436	This work(cal.)
IrW	B19-MgCd	Pmcm	4.452	2.76	4.811	[22]
			4.486	2.788	4.866	This work(cal.)
W	cubic	Im $\bar{3}$ m	3.165	3.165	3.165	[25]
			3.174	3.174	3.174	This work(cal.)

quasirandom structure (SQS) approaches [35, 36]. 16 atoms per unit cell of Ir$_x$Mo$_{1-x}$ and Ir$_x$W$_{1-x}$ (x=0.0625, 0.125, 0.1875, 0.25, 0.5, 0.75, 0.8125, 0.875 and 0.9375) were used for the VASP calculations [37, 38].

4. Thermodynamic model
4.1 Solution phases

In the Ir-M (M = Mo, W) binary systems, the Gibbs free energies of the Liquid, Bcc_A2 and Fcc_A1 phases can be described by the substitutional solution model as follows:

$$G_m^\varphi = \sum_{i=Ir,M} {}^0G_i^\varphi x_i + RT \sum_{i=Ir,M} x_i \ln x_i + \Delta^E G_m^\varphi \tag{2}$$

Where x_i is the mole fraction of the component I, R is the gas constant, and T is the absolute temperature. Here ${}^0G_i^\varphi$ are the Gibbs free energies in the respective reference states of the pure elements that are taken from the SGTE compiled by Dinsdale [39] and described by the following equation:

$$
\begin{aligned}
{}^0G_i^\varphi(T) - H_i^{SER} &= A + B \cdot T + C \cdot T \cdot \ln \cdot T + \\
&D \cdot T^2 + E \cdot T^{-1} + F \cdot T^3 + I \cdot T^7 + J \cdot T^{-9}
\end{aligned}
\tag{3}
$$

Table 2. *Experimental invariant reactions compared with the calculated results of the Ir-Mo and Ir-W systems*
* This reaction is assessed as Liquid+ Ir_3Mo = ε [22].

Reaction	T [ºC]		Phases	Composition	
	Exp	Cal		Exp	Cal
Ir-Mo binary system:				at.% Ir	
L + Fcc_A1 = Ir_3Mo	2300±20	2293	L	—	72.64
			Fcc_A1	78	78.16
			Ir_3Mo	76	75.9
L = ε + Ir_3Mo*	—	2269	L	—	69.87
			ε	—	68.8
			Ir_3Mo	—	74.84
Bcc_A2 + L = $IrMo_3$	2110±10	2116	Bcc_A2	16	15.56
			L	—	24.27
			$IrMo_3$	23	22.12
L + $IrMo_3$ = σ	2095±15	2089	L	—	28.37
			$IrMo_3$	23	23.64
			σ	29	28.33
L = σ + ε	2080±5	2083	L	31	30.73
			σ	29	28.33
			ε	37	38.22
σ = ε + $IrMo_3$	1975±5	1978	σ	29	28.33
			ε	38.5	39.32
			$IrMo_3$	25	24.64
ε = IrMo + Ir_3Mo	—	1491	ε	—	53.61
			IrMo	—	50
			Ir_3Mo	—	62.44
ε = IrMo + $IrMo_3$	—	1477	ε	—	45.63
			IrMo	—	50
			$IrMo_3$	—	25.83
$IrMo_3$ = IrMo + Bcc_A2	—	391	$IrMo_3$	—	24.76
			IrMo	—	50
			Bcc_A2	—	0.11
Ir-W binary system:				at.% W	
L = ε + Fcc_A1	2305±25	2306	L	21	21.01
			ε	~22	23.66
			Fcc_A1	~19	18.94
L = ε + σ	2460±25	2455	L	~70	67.35
			ε	~66	60.07
			σ	~75	74.35
Bcc_A2 + L = σ	2540	2573	Bcc_A2	~90	94.03
			L	~74	70.8
			σ	~75	80
σ = ε + Bcc_A2	1810	1802	σ	75	75.05
			ε	57	56.22
			Bcc_A2	96	95.31
Fcc_A1 + ε = Ir_3W	—	1648	Fcc_A1	—	20.92
			ε	—	24.01
			Ir_3W	—	22.31
ε = IrW + Bcc_A2	—	1575	IrW	—	49.68
			Bcc_A2	—	96.81
			ε	—	54.44
ε = IrW + Ir_3W	—	1234	ε	—	37.41
			IrW	—	47.92
			Ir_3W	—	33.63

in which H_i^{SER} is the molar enthalpy of the element i at 298.15 K and 1 bar in its standard element reference (SER) state. The term on the right of the Eq. (2) is the excess Gibbs free energy, $\Delta^E G_m^{\varphi}$, which is expressed by the Redlich-Kister polynomial [40] :

$$\Delta^E G_m^{\varphi} = x_{Ir} x_M \sum_{m=0}^{n} {}^m L_{Ir,M}^{\varphi} (x_{Ir} - x_M)^m \qquad (4)$$

$${}^m L_{Ir,M}^{\varphi} = a + bT \qquad (5)$$

Eq. (5) is the binary interaction parameters and the coefficients of a and b are parameters to be optimized based on the available experimental data.

4.2 Intermetallic compounds

The intermetallic compounds of the Ir-Mo and Ir-W binary systems are all described by the two-sublattice models [41]. The occupation of atoms in this model can be written as, $(Ir,M)_x(Ir,M)_y$, where the subscripts of x and y represent the number of sites in each sublattice. The Gibbs free energy of the φ phase per mole-formula can be expressed by the following equation:

$$\begin{aligned}
{}^0 G^{\varphi} &= {}^0 G_{Ir:Ir}^{\varphi} \cdot y_{Ir}' \cdot y_{Ir}'' + {}^0 G_{Ir:M}^{\varphi} \cdot y_{Ir}' \cdot y_M'' + \\
&\quad {}^0 G_{M:Ir}^{\varphi} \cdot y_M' y_{Ir}'' + {}^0 G_{M:M}^{\varphi} \cdot y_M' \cdot y_M'' \\
&\quad + x \cdot RT \cdot (y_{Ir}' \ln y_{Ir}' + y_M' \ln y_M') + \\
&\quad y \cdot RT \cdot (y_{Ir}'' \ln y_{Ir}'' + y_M'' \ln y_M'') \\
&\quad + y_{Ir}' y_{Ir}'' y_M'' \, {}^0 L_{Ir:Ir,M}^{\varphi} + y_M' y_{Ir}'' y_M'' \, {}^0 L_{M:Ir,M}^{\varphi} \\
&\quad + y_{Ir}' y_M' y_{Ir}'' \, {}^0 L_{Ir,M:Ir}^{\varphi} + y_{Ir}' y_M' y_M'' \, {}^0 L_{Ir,M:M}^{\varphi} + \cdots
\end{aligned} \qquad (6)$$

Where the parameter y_i^j presents the site fraction of the species i (i= Mo or W) on the sublattice j (j= ' or ''). The superscripts ' and '' denote the first and second sublattice in the present model, respectively. ${}^0 G_{Ir:Ir}^{\varphi}, {}^0 G_{Ir:M}^{\varphi}, {}^0 G_{M:Ir}^{\varphi}$ an ${}^0 G_{M:M}^{\varphi}$ are the Gibbs energy of the end-members which are described similar to the stoichiometric compounds like the IrMo and σ phases in the Ir-Mo binary system. The Gibbs free energies per mole of formula unit for Ir_mMo_n can be written in the following form:

$${}^0 G_{Ir:Mo}^{Ir_mMo_n} = m\,{}^0 G_{Ir}^{fcc} + n\,{}^0 G_W^{bcc} + \Delta\,{}^0 G_f^{Ir_mMo_n} \qquad (7)$$

Here $\Delta\,{}^0 G_f^{Ir_mMo_n}$ indicates the standard Gibbs free energy of formation of the stoichiometric compound from the pure elements, which is expressed as:

$$\Delta\,{}^0 G_f^{Ir_mMo_n} = a' + b'T \qquad (8)$$

The subscripts m and n indicate the ratio of stoichiometry. The coefficient a' and b' in the Eq. (8) are evaluated in the present work.

4.3 Optimization

The thermodynamic model parameters of the Ir-Mo and Ir-W binary systems were evaluated on the basis of experimental information and assessed data using the PARROT module of Thermo-Calc software [42]. The step-by-step optimization procedure described by Du et al. [43] was utilized. Taking the Ir-Mo system as an example, the binary interaction parameters for the liquid phase, ${}^0 L_{Ir,Mo}^{Liq}, {}^1 L_{Ir,Mo}^{Liq}$ and ${}^2 L_{Ir,Mo}^{Liq}$ were firstly introduced to make the liquidus fit better with the melting points and eutectic reaction [15]. Next, the parameters of the solid solutions, ${}^0 L_{Ir,Mo:VA}^{FCC\_A1}, {}^1 L_{Ir,Mo:VA}^{FCC\_A1}, {}^0 L_{Ir,Mo:VA}^{BCC\_A2}$ and ${}^1 L_{Ir,Mo:VA}^{BCC\_A2}$, were optimized by using the mixing enthalpies calculated by SQS models. Then, the formation enthalpies of the intermediate phases were introduced with the two-sublattice model. The parameters b' of the compounds were adjusted to describe the invariant reactions. Finally, all the parameters were evaluated together to provide the best description of the system. The assessed thermodynamic parameters are listed in Table 3.

5. Results and discussions
5.1 The Ir-Mo binary system

The first-principles calculated lattice parameters of the pure Ir, Mo, and intermetallic compounds are shown in Table 1, in which the relative error range between the calculated value and literature data [15, 22, 24] is ±1.20%. The result shows that the error is acceptable. Fig. 1(a) shows the calculated lattice parameters of Fcc_A1 and Bcc_A2 by the SQS approach compared with the experimental data [15]. The relative error range of this phases is ±1.03%. The calculated atomic volumes compared with the experimental data [15] is shown in Fig. 1(b) and the relative error range is ±2.29%. All the calculated results agree well with the experimental ones [15]. Fig. 2(a) shows the mixing enthalpies of Fcc_A1 and Bcc_A2 in the Ir-Mo binary system with the SQS approach and the CALPHAD method. The optimized mixing enthalpies accord well with the SQS models. The formation enthalpies of the Ir-Mo phases are presented in Fig. 2(b), in which the scattered points are the data obtained by the first-principles calculations. The CALPHAD results differ ±4.72kJ/mol-atoms from the first-principles data, which is reasonable agreement. The optimized phase diagram of Ir-Mo is shown in Fig. 3(a). The maximum solubility of Ir in (Mo) and Mo in (Ir) was calculated to be 15.56 at.% at 2116 °C and 21.84 at.% at 2293 °C, respectively. The compositions of the σ and IrMo₃ phases are very close, and thus an enlarged diagram is presented in Fig. 3(b). Fig. 3(c) exhibits the calculated phase diagram compared with the experimental data [15]. The measured data of the phase boundary between Fcc_A1 and Ir₃Mo have an error of 25 °C, which is a large

Table 3. *Summary of the thermodynamic parameters in the Ir-Mo and Ir-W binary systems optimized in the present work.*

Phase	Thermodynamic parameters (J/mol)
Ir-Mo binary system:	
Liquid:(Ir, Mo)$_1$	$^0L_{Ir,Mo}^{Liq}$ = -102800+0.20004T
	$^1L_{Ir,Mo}^{Liq}$ = -25020
	$^2L_{Ir,Mo}^{Liq}$ = -20004+3.0021T
Fcc_A1:(Ir,Mo)$_1$(VA)$_1$	$^0L_{Ir,Mo:VA}^{FCC\_A1}$ = -115046+10.60318T
	$^1L_{Ir,Mo:VA}^{FCC\_A1}$ = -20000-20.9T
Bcc_A2:(Ir,Mo)$_1$(VA)$_3$	$^0L_{Ir,Mo:VA}^{BCC\_A2}$ = -50015-21.0063T
	$^1L_{Ir,Mo:VA}^{BCC\_A2}$ = -48028.8
σ: (Ir)$_{17}$(Mo)$_{43}$	$^0G_{Ir:Mo}^{\sigma}$ = 17G$_{Ir}^{fcc}$+43G$_{Mo}^{bcc}$-244000-509.3T
Ir$_3$Mo:(Ir,Mo)$_3$(Ir,Mo)$_1$	$^0G_{Ir:Ir}^{Ir_3Mo}$ = 4^{0}G$_{Ir}^{fcc}$+80024
	$^0G_{Ir:Mo}^{Ir_3Mo}$ = 3^{0}G$_{Ir}^{fcc}$ + $^0G_{Mo}^{bcc}$-122261.1
	$^0G_{Mo:Ir}^{Ir_3Mo}$ = 3$^0G_{Mo}^{bcc}$+^{0}G$_{Ir}^{fcc}$+40004
	$^0G_{Mo:Mo}^{Ir_3Mo}$ = 4$^0G_{Mo}^{bcc}$+86008.6
	$^0L_{Ir,Mo:Ir}^{Ir_3Mo}$ = -200080+39T
	$^0L_{Ir,Mo:Mo}^{Ir_3Mo}$ = -200080+39T
	$^0L_{Ir:Ir,Mo}^{Ir_3Mo}$ = -108054
	$^0L_{Mo:Ir,Mo}^{Ir_3Mo}$ = -108054
IrMo$_3$:(Ir,Mo)$_1$(Ir,Mo)$_3$	$^0G_{Ir:Ir}^{IrMo_3}$ = 4^{0}G$_{Ir}^{fcc}$+15001.5
	$^0G_{Ir:Mo}^{IrMo_3}$ = ^{0}G$_{Ir}^{fcc}$+3$^0G_{Mo}^{bcc}$-40032-18.91512T
	$^0G_{Mo:Ir}^{IrMo_3}$ = $^0G_{Mo}^{bcc}$+3^{0}G$_{Ir}^{fcc}$+80008
	$^0G_{Mo:Mo}^{IrMo_3}$ = 4$^0G_{Mo}^{bcc}$+36390
	$^0L_{Ir,Mo:Ir}^{IrMo_3}$ = -12009.6
	$^0L_{Ir,Mo:Mo}^{IrMo_3}$ = -12009.6
	$^0L_{Ir:Ir,Mo}^{IrMo_3}$ = -45036
	$^0L_{Mo:Ir,Mo}^{IrMo_3}$ = -45036
IrMo:(Ir)$_1$(Mo)$_1$	$^0G_{Ir:Mo}^{IrMo}$ = ^{0}G$_{Ir}^{fcc}$ + $^0G_{Mo}^{bcc}$-49004.9-5.5T
ε:(Ir,Mo)$_1$(Ir,Mo)$_1$	$^0G_{Ir:Ir}^{\varepsilon}$ = 2^{0}G$_{Ir}^{fcc}$+2000.2
	$^0G_{Ir:Mo}^{\varepsilon}$ = ^{0}G$_{Ir}^{fcc}$ + $^0G_{Mo}^{bcc}$-40028.01-7T
	$^0G_{Mo:Ir}^{\varepsilon}$ = $^0G_{Mo}^{bcc}$+^{0}G$_{Ir}^{fcc}$-40028.01-7T
	$^0G_{Mo:Mo}^{\varepsilon}$ = 2^{0}G$_{Mo}^{bcc}$+103010.3-25T
	$^0L_{Ir,Mo:Ir}^{\varepsilon}$ = -50101-3.1T
	$^0L_{Ir,Mo:Mo}^{\varepsilon}$ = -50101-3.1T
	$^0L_{Mo:Ir,Mo}^{\varepsilon}$ = -70011+10.011T
	$^0L_{Ir:Ir,Mo}^{\varepsilon}$ = $-70011+10.011T$

*table continues on the next line

*table continued from the previous line

Ir-W binary system:	
Liquid:(Ir, W)$_1$	$^0L_{Ir,W}^{Liq}$ = -105000
	$^1L_{Ir,W}^{Liq}$ = -42000+T
	$^2L_{Ir,W}^{Liq}$ = -20000
Fcc_A1:(Ir, W)$_1$(VA)$_1$	$^0L_{Ir,W:VA}^{FCC\_A1}$ = -94000+5T
	$^1L_{Ir,W:VA}^{FCC\_A1}$ = -65000-8T
Bcc_A2:(Ir, W)$_1$(VA)$_3$	$^0L_{Ir,W:VA}^{BCC\_A2}$ = -40000-7.2T
	$^1L_{Ir,W:VA}^{BCC\_A2}$ = -35000
Ir$_3$W:(Ir, W)$_3$(Ir, W)$_1$	$^0G_{Ir:Ir}^{Ir_3W}$ = 4^{0}G$_{Ir}^{fcc}$+29200
	$G_{Ir:W}^{Ir_3W}$ = 3^{0}G$_{Ir}^{fcc}$+G$_W^{bcc}$-108550+2T
	$G_{W:Ir}^{Ir_3W}$ = 3^{0}G$_W^{bcc}$+^{0}G$_{Ir}^{fcc}$+44000
	$^0G_{W:W}^{Ir_3W}$ = 4$^0G_W^{bcc}$+220000
	$^0L_{Ir,W:Ir}^{Ir_3W}$ = -290000
	$^0L_{Ir,W:W}^{Ir_3W}$ = -290000
	$^0L_{Ir:Ir,W}^{Ir_3W}$ = -75000
	$^0L_{W:Ir,W}^{Ir_3W}$ = -75000
IrW:(Ir)$_1$(Ir,W)$_1$	$^0G_{Ir:Ir}^{IrW}$ = 2^{0}G$_{Ir}^{fcc}$+14000
	$^0G_{Ir:W}^{IrW}$ = $^0G_W^{bcc}$ + ^{0}G$_{Ir}^{fcc}$-45000-5T
	$^0L_{Ir:Ir,W}^{IrW}$ = -39000
ε:(Ir, W)$_1$(Ir, W)$_1$	$^0G_{Ir:Ir}^{\varepsilon}$ = 2^{0}G$_{Ir}^{fcc}$+13500
	$^0G_{Ir:W}^{\varepsilon}$ = ^{0}G$_{Ir}^{fcc}$+^{0}G$_W^{bcc}$-45000
	$^0G_{W:Ir}^{\varepsilon}$ = ^{0}G$_W^{bcc}$ + ^{0}G$_{Ir}^{fcc}$+120000+12T
	$^0G_{W:W}^{\varepsilon}$ = 2^{0}G$_W^{bcc}$+100000
	$^0L_{Ir:Ir,W}^{\varepsilon}$ = -100000-6T
	$^0L_{Ir,W:Ir}^{\varepsilon}$ = -100000-6T
	$^0L_{Ir,W:W}^{\varepsilon}$ = 10000-65T
	$^0L_{W:Ir,W}^{\varepsilon}$ = 10000-65T
	$^1L_{Ir,W:Ir}^{\varepsilon}$ = -38000
	$^1L_{Ir:Ir,W}^{\varepsilon}$ = -38000
σ:(Ir, W)$_1$(Ir, W)$_3$	$^0G_{Ir:Ir}^{\sigma}$ = 4^{0}G$_{Ir}^{fcc}$
	$^0G_{Ir:W}^{\sigma}$ = ^{0}G$_{Ir}^{fcc}$+3$^0G_W^{bcc}$+4500-25.7T
	$^0G_{W:Ir}^{\sigma}$ = $^0G_W^{bcc}$+3^{0}G$_{Ir}^{fcc}$-15000+90T
	$^0G_{W:W}^{\sigma}$ = 4$^0G_W^{bcc}$+35839
	$^0L_{Ir,W:Ir}^{\sigma}$ = 10000-16T
	$^0L_{Ir,W:W}^{\sigma}$ = 10000-16T
	$^0L_{Ir:Ir,W}^{\sigma}$ = -51000-38T
	$^0L_{W:Ir,W}^{\sigma}$ = -51000-38T

uncertainty [15]. Therefore, these data were set a lower weight in the optimization. Nine invariant reactions were calculated, including, Liquid + Fcc_A1 = Ir$_3$Mo, Liquid = ε + Ir$_3$Mo, Bcc_A2 + Liquid = IrMo$_3$, Liquid + IrMo$_3$ = σ, Liquid = σ + ε, σ = ε + IrMo$_3$, ε = IrMo + Ir$_3$Mo, ε = IrMo + IrMo$_3$ and IrMo$_3$ = IrMo + Bcc_A2. In Fig. 4(a), the peritectic reaction Liquid + Ir$_3$Mo = ε assessed by Giessen et al. [22] which appears in the high-temperature range above 2100 ºC is replaced by a eutectic reaction Liquid = ε + Ir$_3$Mo in the present work. The calculated reaction can be regarded as tentative because no experimental information can verify the reaction type [22]. Moreover, they assumed the existence of two eutectoid reactions, i.e., ε = IrMo + Ir$_3$Mo and ε = IrMo + IrMo$_3$, analogy to the Mo-Pt system [44]. The temperatures of these eutectoid transformations were predicted to be 1491 ºC and 1477 ºC, respectively. In table 2, a summary of the invariant equilibria of the binary Ir-Mo system is given to compare with the experimental and optimized temperatures and compositions.

5.2 The Ir-W binary system

The comparison of the lattice parameters between the calculated results and the experimental data of Ir-W is shown in Table 1, with the relative error range of ±2.63%, which is a good agreement. Fig. 4(a) shows the mixing enthalpies of Fcc_A1 and Bcc_A2 calculated by the SQS approach and CALPHAD method. The formation enthalpies of the compounds calculated by the first-principles calculations can be seen in Fig. 4(b), which were used as the initial values for the optimization. The optimized mixing enthalpies have a good agreement with the SQS models. Fig. 5(a) shows the optimized phase diagram of Ir-W, which includes seven invariant reactions: Liquid = ε + Fcc_A1, Liquid = ε + σ, Bcc_A2 + Liquid = σ, σ = ε + Bcc_A2, Fcc_A1 + ε = Ir$_3$W, ε = IrW + Bcc_A2 and ε = IrW + Ir$_3$W. In the present work, the peritectic reaction, Bcc_A2 + Liquid = σ, was given a lower weight than the eutectoid reaction at 1810 ºC due to the large uncertainty of the experimental data. The comparison of invariant equilibria between the experimental data [14, 16, 17, 20] and the calculated results are listed in Table 2. Further comparison between the experimental data [14, 16, 17, 20] and the calculated results is shown in Fig. 5(b). It is indicated that the experimental phase equilibria data can be reproduced by the present CALPHAD-type calculations.
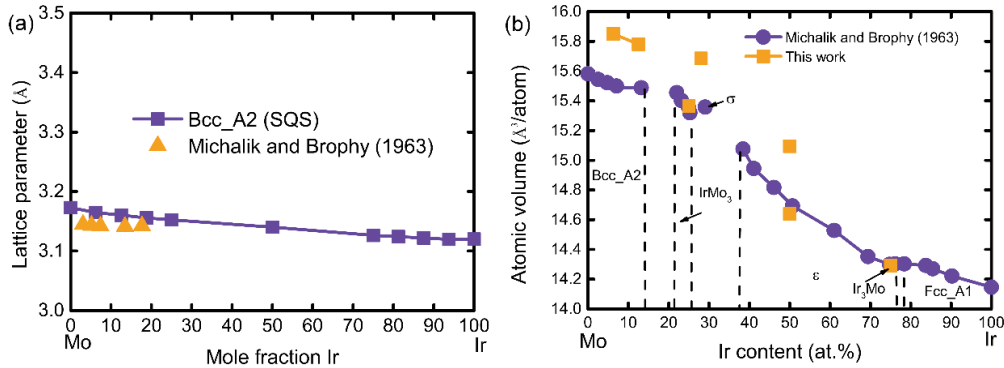
Figure 1. Lattice parameters of the Ir-Mo system: (a) the obtained results of Bcc_A2 by the first-principles calculations compared with the experimental data [15]; (b) the calculated atomic volumes compared with the experimental data [15]
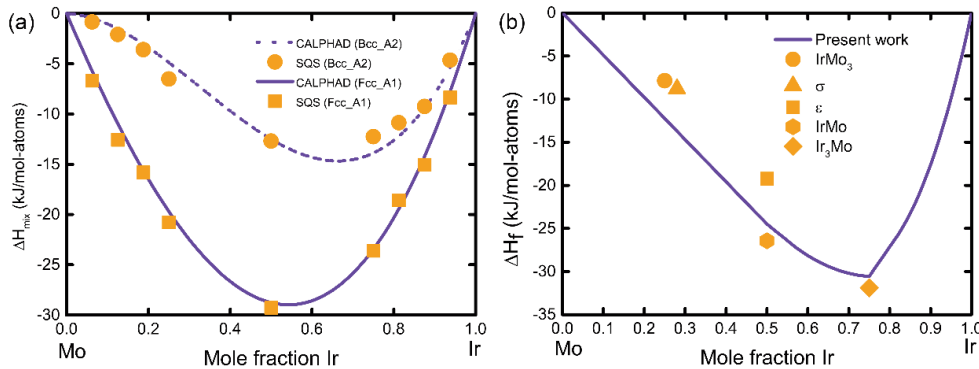
Figure 2. Thermodynamic data of the Ir-Mo system: (a) mixing enthalpies of Fcc_A1 and Bcc_A2 calculated by the CALPHAD (at 298 K) and SQS (at 0 K) approaches; (b) formation enthalpies obtained by the CALPHAD (at 298 K) and the first-principles (at 0 K) calculations
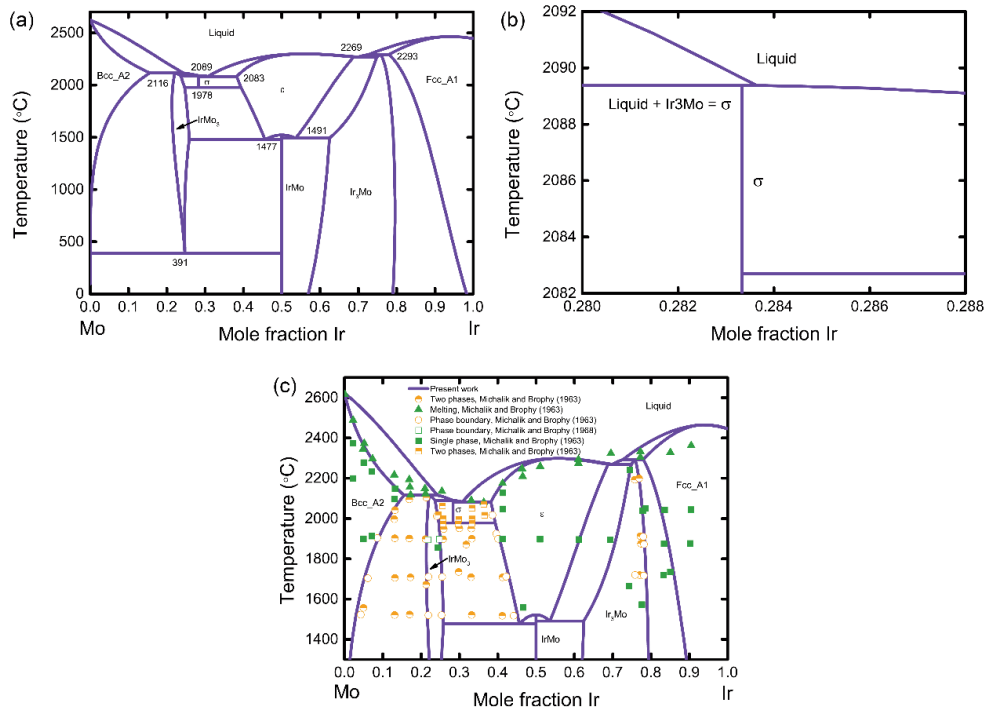
Figure 3. *The calculated Ir-Mo phase diagram: (a) without experimental data; (b) enlarged one with the invariant reaction Liquid + IrMo₃ = σ; (c) with the experimental data [15]*
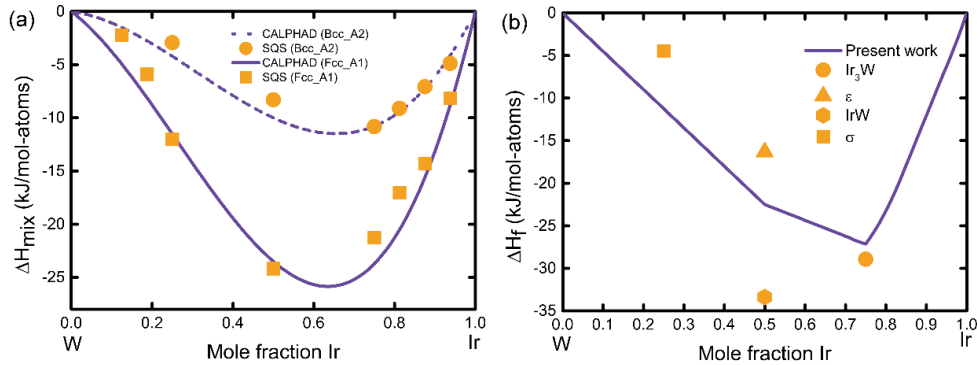
Figure 4. *Thermodynamic data of the Ir-W system: (a) mixing enthalpies of Fcc_A1 and Bcc_A2 calculated by the CALPHAD (at 298 K) and SQS (at 0 K) approaches; (b) formation enthalpies obtained by the CALPHAD (at 298 K) and the first-principles (at 0 K) calculations*
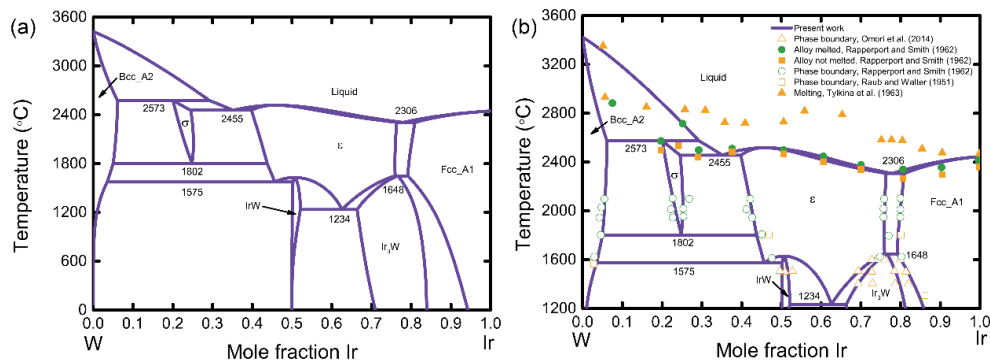
Figure 5. *The calculated Ir-W phase diagram: (a) without experimental data; (b) with the experimental data [13, 14, 16, 17]*

6. Conclusions

The lattice parameters calculated by the first-principles calculations accord well with the experimental data, which demonstrates that the calculations are reliable. Formation enthalpies of the compounds and end-members calculated by the first-principles calculations were used as an input during the CALPHAD-type optimization.

A set of self-consistent thermodynamic parameters of the Ir-Mo and Ir-W systems were obtained by the CALPHAD approach. All the reliable experimental information can be satisfactorily reproduced by the present optimized parameters.

Acknowledgments

References

[1] R. Weiland, D.F. Lupton, B. Fischer, J. Merke, C. Scheckenbach, J. Witte, Platinum Metals Rev., 50 (2006) 13.

[2] Y. Liu, C.T. Liu, L. Heatherly, J. Alloy. Compd. 459 (2008) 5.

[3] E.K. Ohriner, Platinum Metals Rev., 52 (2008) 12.

[4] B.L. Mordike, C.A. Brookes, Platinum Metals Rev., 4 (1960) 6.

[5] OH, Metals Handbook, 9nd ed., Metals Park, USA, 1979.

[6] S.S. Hecker, D.L. Rohr, D.F. Stein, , Metall. Tran. A, 9A (1978) 1.

[7] D.L. Rohr, L.E. Murr, S.S. Hecker, Metall.Tran. A, 10A (1979) 2.

[8] C.T. Liu, H. Inouye, A.C. Schaffhauser, Metallurgical Transactions A, 12A (1981) 1.

[9] A. Luo, D.L. Jacobson, K.S. Shin, Int. J. of Refract. Met. Hard Mater., 10 (1991) 8.

[10] Y. Yamabe-Mitarai, H. Murakami, Intermetallics, 48 (2014) 7.

[11] A.G. Knapton, Platinum Metals Rev., 24 (1980) 6.

[12] E.K. Ohriner, W. Zhang, G.B. Ulrich, Int. J. of Refract. Met. Hard Mater., 35 (2012) 5.

[13] E. raub, P. Walter, Alloys of the platinum-group metals with tungsten, Heraeus Festschr, (1951) 23.

[14] E.J. Rapperport, M.F. Smith, Tech. rept. WADD-TR-60-132. Pt. II, (1962) 15.

[15] S.J. Michalik, J.H. Brophy, Trans. Metall. Aime, 227 (1963) 7.

[16] M.A. Tylkina, V.P. Polyakova, V.S. Shekhtman, Zh Neorg Khim, 8 (1963) 7.

[17] T. Omori, K. Makino, K. Shinagawa, I. Ohnuma, R. Kainuma, K. Ishida, Intermetallics, 55 (2014) 8.

[18] Z.K. Liu, J. Phase Equilibria Diffus., 30 (2009) 18.

[19] A.K. Mallik, Buff. Mater. Sci., 8 (1986) 15.

[20] E. Raub, Z. Metallk., 45 (1954) 1.

[21] A.G. Knapton, J. Inst. Met., 87 (1958) 5.

[22] B.C. Giessen, U. Jaehnigen, N.J. Grant, J. Less-Common Metals, 10 (1965) 2.

[23] S.V. Nagender Naidu, A.M. Sriramamurthy, P. Rama Rao, Indian Institute of Metals, (1991) 7.

[24] F.J. Spooner, Acta Cryst., 17 (1964) 6.

[25] W.K. Goetz, J.H. Brophy, J. Less-Common Metals, 6 (1964) 9.

[26] Y. Wang, S. Curtarolo, C. Jiang, CALPHAD, 28 (2004) 12.

[27] Y. Zhong, C. Wolverton, Y. Austin Chang, Acta Mater., 52 (2004) 16.

[28] K.K. Chang, Y. Du, W. Sun, CALPHAD, 34 (2010) 6.

[29] Z.X. Deng, D.P. Zhao, Y.Y. Huang, J. Min. Metall. Sect. B-Metall., 55 (2019) 11.

[30] G. Kresse, J. Furthmüller, Phys. Rev. B Condens. Matter, 54 (1996) 18.

[31] J.P. Perdew, K. Burke, M. Ernzerhof, Physical Review Letters, 77 (1996) 4.

[32] J.P. Perdew, J. Chevary, S. Vosko, Phys. Rev. B Condens. Matter, 46 (1992) 17.

[33] G. Kresse, D. Joubert, Phys. Rev. B Condens. Matter, 59 (1999) 18.

[34] H.J. Monkhorst, J.D. Pack, PPhys. Rev. B Condens. Matter, 13 (1972) 5.

[35] A. Zunger, S.H. Wei, L.G. Ferreira, J.E. Bernard, Phys. Rev. Lett., 65 (1990) 4.

[36] C. Jiang, C. Wolverton, J. Sofo, Phys. Rev. B Condens. Matter, 69 (2004) 10.

[37] K. Chang, M.t. Baben, D. Music, Acta Mater., 98 (2015) 6.

[38] K. Chang, D. Music, M.t. Baben, Sci. Technol. Adv. Mater., 17 (2016) 10.

[39] A.T. Dinsdale, SGTE data for pure elements, CALPHAD, 15 (1991) 109.

[40] O. Redlich, A.T. Kitster, Ind. Eng. Chem, 40 (1948) 4.

[41] H. Hillert, L.I. Stafansson, Acta Chem. Scand, 24 (1970) 7.

[42] J.O. Andersson, T. Helander, L. Höglund, CALPHAD, 26 (2002) 40.

[43] Y. Du, R. Schmid-Fetzer, H. Ohtani, Z. Metallkd, 88 (1997) 12.

[44] A. Raman, K. Schubert, Z. Metallk., 55 (1964) 1.

ISPITIVANJE Ir-Mo I Ir-W SISTEMA KORIŠĆENJEM METODA PRVOG PRINCIPA I CALPHAD

Y.-Y. Huang [a,b], B. Wu [a,*], F. Li [c,*], L.-L. Chen [b], Z.-X. Deng [b], K. Chang [b]

[a] Postrojenje za višeskalne računske materijale, Fakultet za nauku o materijalima i inženjerstvo, Univerzitet u Fuzhou, Fuzhou, NR Kina
[b] Inženjerska laboratorija za materijale napredne energije, Ningbo institut za tehnologiju materijala i inženjerstvo, Kineska akademija nauka, Ningbo, Zeidžang, NR Kina
[c] Fakultet za nauku o materijalima i inženjerstvo, Jiao Tong univerzitet u Šangaju,Šangaj, NR Kina

Apstrakt

U ovoj studiji je predstavljeno termodinamičko modeliranje Ir-Mo i Ir-W sistema uz korišćenje CALPHAD (proračun faznih dijagrama) pristupa podržanog proračunima prvog principa. Za oba sistema u literaturi je izvršena kritička procena fazne ravnoteže i podataka o termodinamičkim osobinama. Usled nedostatka eksperimentalnih podataka, primenjeni su proračuni prvog principa da bi se dobile entalpije čvrstih i intermetalnih faza. Termodinamički parametri procenjeni su korišćenjem PARROT modula Thermo-Calc softvera. Posle optimizacije dobijen je skup doslednih parametara za Ir-Mo i Ir-W sisteme. Postignuto je zadovoljavajuće slaganje između proračunatih rezultata i eksperimentalnih podataka, uključujući faznu ravnotežu i termodinamičke osobine.

Ključne reči: CALPHAD; Ir-Mo; Ir-W; Fazni dijagram; Proračuni prvog principa